Hematopoietic Stem Cell Gene Therapy for the Multisystemic Lysosomal Storage Disorder Cystinosis

Frank Harrison[1], Brian A Yeagy[1], Celine J Rocca[1], Donald B Kohn[2,3], Daniel R Salomon[1] and Stephanie Cherqui[1]

[1]Department of Molecular and Experimental Medicine, The Scripps Research Institute, La Jolla, California, USA; [2]Department of Microbiology, Immunology and Molecular Genetics, University of California, Los Angeles, California, USA; [3]Department of Pediatrics, University of California, Los Angeles, California, USA

Cystinosis is an autosomal recessive metabolic disease that belongs to the family of lysosomal storage disorders (LSDs). The defective gene is *CTNS* encoding the lysosomal cystine transporter, cystinosin. Cystine accumulates in all tissues and leads to organ damage including end-stage renal disease. Using the *Ctns*$^{-/-}$ murine model for cystinosis, we tested the use of hematopoietic stem and progenitor cells (HSPC) genetically modified to express a functional *CTNS* transgene using a self-inactivating-lentiviral vector (SIN-LV). We showed that transduced cells were capable of decreasing cystine content in all tissues and improved kidney function. Transduced HSPC retained their differentiative capabilities, populating all tissue compartments examined and allowing long-term expression of the transgene. Direct correlation between the levels of lentiviral DNA present in the peripheral blood and the levels present in tissues were demonstrated, which could be useful to follow future patients. Using a new model of cystinosis, the DsRed *Ctns*$^{-/-}$ mice, and a LV driving the expression of the fusion protein cystinosin-enhanced green fluorescent protein (eGFP), we showed that cystinosin was transferred from CTNS-expressing cells to Ctns-deficient adjacent cells *in vitro* and *in vivo*. This transfer led to cystine decreases in Ctns-deficient cells *in vitro*. These data suggest that the mechanism of cross-correction is possible in cystinosis.

Received 27 June 2012; accepted 16 September 2012; advance online publication 23 October 2012. doi:10.1038/mt.2012.214

INTRODUCTION

Numbers of reports have established a proof-of-principle for allogeneic hematopoietic stem and progenitor cell (HSPC) transplantation in several lysosomal storage disorders (LSDs).[1] However, a suitable hematopoietic donor is not always found and the risk of morbidity and mortality associated with allogeneic transplantation is significant. The major complication is graft-versus-host disease (GVHD).[2,3] In recent studies, acute GVHD grade II–IV occurred in 20–32% of patients and chronic GVHD in 16–59%, both significantly impacting survival of the recipients.[4–6] Moreover, high risks of infection related to the myeloablative regimen and immunosuppressive medications account for 16–19% of deaths.[7,8] Thus, even though the risk/benefit ratio of allogeneic hematopoietic stem cell (HSC) transplantation still favors selected LSDs, it remains an uncertain therapeutic choice for others. In contrast, autologous HSPC transplantation, if successful, would greatly expand the opportunities to apply this strategy in any LSD because it avoids the risks of GVHD and may be done with a reduced intensity myeloablative regimen.

Cystinosis is an LSD that could benefit from autologous gene-modified HSPC transplantation. Since the introduction and regular use of the drug cysteamine, many patients may live to adulthood but with significant medical problems and the mean age of death is around 28 years old.[9] Cystinosis is characterized by lysosomal accumulation of cystine, which leads to the formation of cystine crystals and multiple organ dysfunction and progressive degeneration. The gene underlying cystinosis, *CTNS*, encodes a seven transmembrane domain protein, cystinosin, a lysosomal cystine transporter.[10–12] Affected individuals typically present before 2 years of age with a De Toni-Debré-Fanconi syndrome characterized by a proximal tubulopathy and progress to end-stage renal failure; they also develop photophobia, hypothyroidism, hypogonadism, diabetes, myopathy, and central nervous system defects.[13] If used early in the disease and in high doses, cysteamine delays the progression of disease.[14] The need for frequent dosing and multiple side effects, render its compliance difficult. Moreover, cysteamine does not prevent the proximal tubulopathy and the end-stage renal failure that occurs in the majority of cystinosis patients before the age of 16.[15]

Using the mouse model for cystinosis, *Ctns*$^{-/-}$ mice,[16] we recently showed that congenic HSPC transplantation from wild-type donors into *Ctns*$^{-/-}$ mice led to significant decreases of cystine in every tissue tested correlating with the abundant tissue integration of bone marrow-derived cells.[17] This treatment also successfully protected these animals from the progression of kidney tissue injury if a relatively high level of donor-derived blood cell engraftment of Ctns-expressing cells was achieved.[18] Thus, this work was the first step towards a clinical trial of using HSPC transplantation as a therapy for cystinosis.

Correspondence: *Stephanie Cherqui, Department of Molecular and Experimental Medicine, The Scripps Research Institute, 10550 North Torrey Pines Road, La Jolla, California 92037, USA. E-mail: scherqui@scripps.edu*

The second step is described in this article by establishing an autologous HSPC transplantation protocol for this disease using a self-inactivating-lentivirus vector (SIN-LV) containing a functional human *CTNS* cDNA. SIN-LVs have shown tremendous benefit as a vehicle for gene delivery as they efficiently transduce many different cell types including stem cells[19–22] and present many safety features.[23–26] Numerous studies have shown the long-term efficacy of lentiviral-transduced hematopoietic cells in mouse models of other LSD.[27–30] Recently, a proof-of-concept for the potential efficacy of SIN-LVs was observed in a clinical trial involving *ex vivo* modified HSC for a peroxisomal storage disorder, X-linked adrenoleukodystrophy.[31] We now report studies on the use of a LV to correct the gene defect in the murine model of cystinosis that will support the first gene and cell therapy clinical trial. Using this strategy to deliver a fusion protein cystinosin-enhanced green fluorescent protein (eGFP) and a new mouse model for cystinosis constitutively expressing a DsRed reporter gene, we also provide new insights into the mechanisms of the long-term therapeutic effects of transplanted HSPC expressing a functional *CTNS* gene.

RESULTS

Lentiviral HSPC transduction as an efficient and stable vehicle for long-term transgene expression within tissues in the cystinosis mouse model

The human *CTNS*, *eGFP*, and luciferase (LUC) cDNA were subcloned in the SIN-LV pCCL-EFS-X-WPRE (pCCL). The constructs pCCL-eGFP and pCCL-LUC were used to optimize transduction of murine Sca1$^+$ HSPC and to monitor the efficiency and stability of transgene expression over time in *Ctns*$^{-/-}$ mice. Freshly isolated wild-type Sca1-enriched cells were transduced with pCCL-eGFP and pCCL-LUC *ex vivo* with LV particles added at multiplicity of infection 5, 10 or 20. Optimal transduction efficiency was obtained with an multiplicity of infection of 10 (data not shown).

Ex vivo transduction efficiency and transgene expression stability were measured *in vivo* either in peripheral blood by flow cytometry to quantify eGFP$^+$ cells or using the IVIS imaging system to quantify luciferase expression in live mice. High levels of eGFP$^+$ cells in the blood of eight transplanted mice were detected, ranging from 26.7 to 93.5% at 4 months post-transplant. Levels were stable up to 9 months post-transplant, which represents the last time point measured for this study (**Figure 1a**). The mean number of eGFP$^+$ cells in the blood of the mice was 70.6 ± 22.0% and the mean contribution for each lineage: 9.6 ± 2.6% T-lymphocytes, 37.0 ± 19.7% B-lymphocytes, and 13.6 ± 7.2% monocytes (**Figure 1b**). The remaining eGFP$^+$ cells were granulocytes. High levels of pCCL-eGFP–transduced bone marrow-derived cells were observed in all the tissues tested including the kidney, liver, spleen, and brain of *Ctns*$^{-/-}$ mice as previously observed for wild-type eGFP HSPC[17,18] (**Figure 2**). These cells strongly expressed eGFP as determined by direct fluorescence and by immunofluorescence staining using an anti-GFP antibody (**Figure 2b**). In addition, we showed that most of the differentiated eGFP-expressing bone marrow-derived cells are Kupffer cells in the liver, microglial cells in the brain, and inflammatory dendritic cells in the kidney, colocalizing with an anti-F4/80 antibody (**Figure 2c–e**) and as shown previously.[17,18] No eGFP-positive cells and no anti-GFP staining were seen in non-transplanted controls (**Figure 2a**). These data showed that *ex vivo* transduction and manipulation of the HSPC did not affect their differentiative capacity.

Finally, high levels of luciferase expression were also observed in eight *Ctns*$^{-/-}$ mice transplanted with pCCL-LUC–transduced HSPC in tissues up to 12 months post-transplantation, the last time point considered for this study (**Figure 1c**). These data showed that *ex vivo* transduced HSPC still efficiently engrafted in tissues in *Ctns*$^{-/-}$ mice and that the transgene was highly expressed for up to a year.

Long-term *in vivo* correction

We are working with the human *CTNS* cDNA and using a vector backbone currently used in clinical trials[31] in these mouse model studies to establish the preclinical proof-of-concept for a human trial. The construct pCCL-CTNS was first verified *in vitro*. Gene transfer of *CTNS* cDNA into murine Ctns$^{-/-}$ fibroblasts led to high expression of *CTNS* transcripts and a significant decrease of cystine compared with pCCL-eGFP–transduced or non-transduced Ctns$^{-/-}$ fibroblast controls (**Figure 3a**). Sca1$^+$ HSPC isolated from *Ctns*$^{-/-}$ mice were transduced *ex vivo* with pCCL-CTNS using an multiplicity of infection of 10 and transplanted into 1–4 months old *Ctns*$^{-/-}$ mice. The rationale for this choice was to be a first proof-of-concept that this strategy of gene-modified HSPC transplantation could work in young patients with cystinosis before significant disease progression. Cystine contents of brain, eye, heart, kidney, liver, muscle, and spleen were analyzed after 4 (group 1; $n = 8$) and 8 (group 2; $n = 12$) months post-transplantation, corresponding to 6–8 months and 9–11 months old mice, respectively. As controls, we used age-matched non-treated *Ctns*$^{-/-}$ mice ($n = 7$ and $n = 12$) or transplanted with wild-type HSPC ($n = 4$ and $n = 4$). Decreases in cystine content were statistically significant in all the tissues tested of mice treated with pCCL-CTNS–transduced HSPC compared with *Ctns*$^{-/-}$ controls except the kidney at 4 months post-transplant and the kidney and eye at 8 months (**Figure 3b**). The levels of decrease observed in *Ctns*$^{-/-}$ mice treated with wild-type syngeneic HSPC were significantly better in most tissues compared to the mice treated with pCCL-CTNS–transduced HSPC except in brain and kidney at 8 months post-transplantation (**Figure 3b**). As previously shown,[17] no benefit was observed in *Ctns*$^{-/-}$ mice transplanted with Ctns$^{-/-}$ HSPC being equivalent to the non-treated mice ($P > 0.05$ for all tissues; data not shown). We also tested the impact of Ctns$^{-/-}$ HSPC transduced with control vector, pCCL-eGFP, on tissue cystine levels to exclude the possibility that the presence of any transgene results in cystine decreases. No decrease in cystine levels in any tissue was observed in *Ctns*$^{-/-}$ mice transplanted with pCCL-eGFP–transduced Ctns$^{-/-}$ HSPC ($n = 2$) compared with non-treated *Ctns*$^{-/-}$ mice ($n = 2$) at 11 months post-transplantation, consistent with the conclusion that cystine decreases obtained in pCCL-CTNS–treated mice are specifically due to the presence of the *CTNS* gene (data not shown).

Curiously, the kidney was the only tissue in which no significant cystine decrease could be consistently obtained with either wild-type or lentiviral-modified HSPC. Comparison of tissue cystine content of non-treated *Ctns*$^{-/-}$ male and female mice revealed

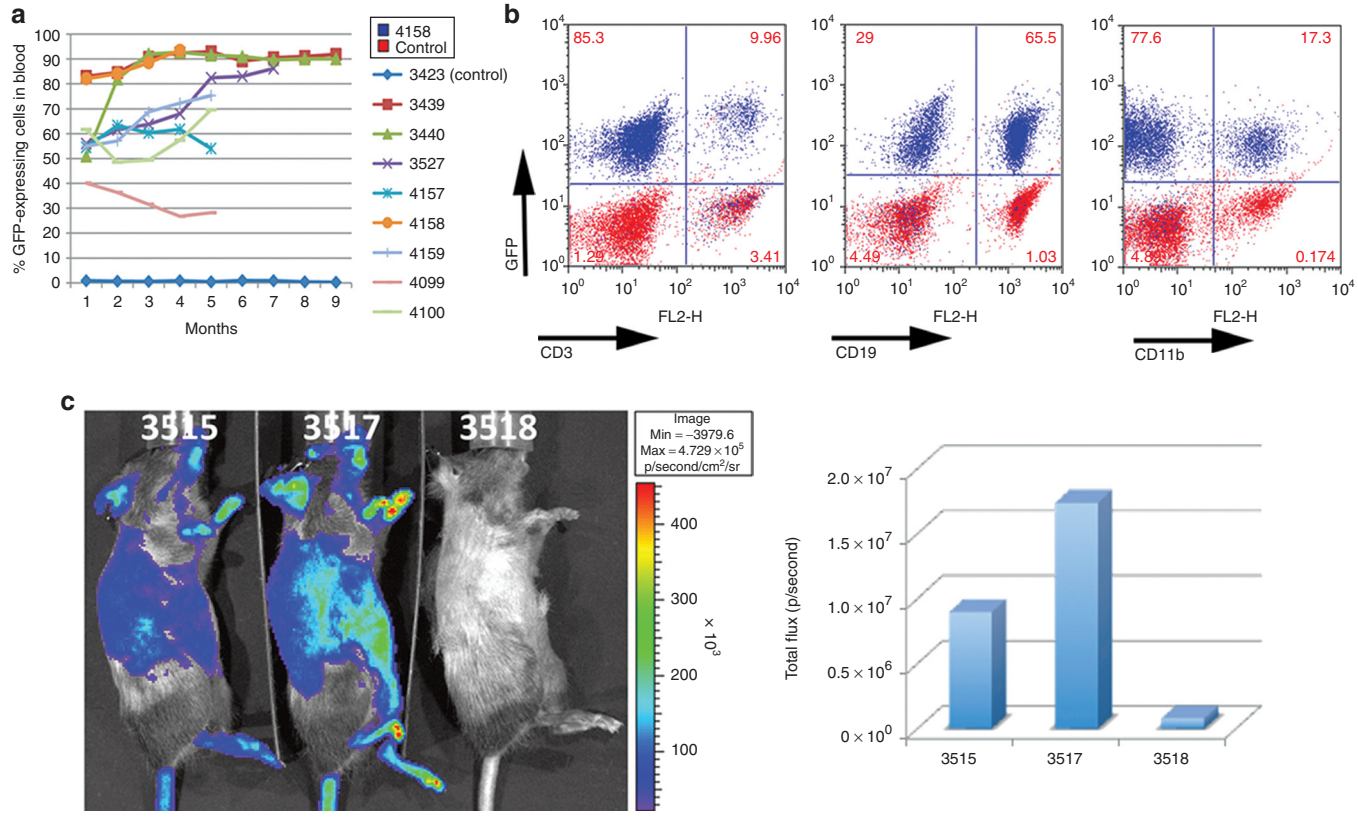

Figure 1 Transduction efficiency and stability of the transgene. (**a**,**b**) Blood cell engraftment in *Ctns*$^{-/-}$ mice transplanted with pCCL-eGFP–transduced HSPC. (**a**) Percentage of eGFP-expressing cells measured in red cell-lysed peripheral blood at different time points in eight *Ctns*$^{-/-}$ mice transplanted with pCCL-eGFP–transduced HSPC (from #3439 to 4100; $n = 8$) and one non-treated *Ctns*$^{-/-}$ mouse control (#3423). The transduction efficiency was over 50% for all the mice except one, even reaching 90% for two of them. eGFP expression was stable for up to 9 months. (**b**) Flow cytometry analysis of the hematopoietic lineage contribution of eGFP-expressing cell in the blood for mouse 4158 compared with a non-transplanted mouse control. Transduced HSPC are capable of generating T-lymphocytes, B-lymphocytes, and monocytes. (**c**) *In vivo* luciferase imaging in *Ctns*$^{-/-}$ mice transplanted with pCCL-LUC–transduced HSPC ($n = 8$). Representative picture of two *Ctns*$^{-/-}$ mice transplanted with pCCL-LUC–transduced HSPC (3515 and 3517) compared with a non-transplanted *Ctns*$^{-/-}$ mouse control (3518) at 12 months post-transplantation. Live animals were injected with luciferin and luciferase expression was acquired using the IVIS imaging system. The luminescence signal intensities (total photon flux) were quantified and represented in the histogram. eGFP, enhanced green fluorescent protein; HSPC, hematopoietic stem and progenitor cell; LUC, luciferase.

that cystine levels were significantly higher in female kidneys than in males (194.91 ± 114.73 in females versus 70.02 ± 23.10 in males; $P < 0.001$). The other tissues did not present such a difference (data not shown). We tested several age groups. After 13 months of age, the difference between males and females in kidney cystine content was no longer observed (data not shown). These new data highlight the fact that males and females have to be analyzed separately for these kidney studies. Thus, we compared kidney cystine content in male *Ctns*$^{-/-}$ mice treated with pCCL-CTNS ($n = 8$) and non-treated controls ($n = 9$) at 8 months post-transplantation. A significant decrease of cystine content in kidney was observed in the treated males (**Figure 3c**). Moreover, quantification of cystine crystals in the kidney sections revealed a significant decrease of crystals in the pCCL-CTNS–treated males compared with non-treated controls (**Figure 4**).

Renal function was assessed by measuring creatinine, urea, and phosphate levels in the serum, and creatinine clearance in 24-hour urine collections in the males at 8 months post-transplant and compared with age-matched wild-type males ($n = 6$). In non-treated *Ctns*$^{-/-}$ mice, the creatinine clearance decreased and all other parameters measured increased compared with wild-type mice (**Table 1**). In the pCCL-CTNS–treated *Ctns*$^{-/-}$ mice, serum creatinine, urine phosphate, and urine volume were significantly decreased compared with non-treated controls, showing a beneficial effect of the genetically modified HSPC on kidney function in *Ctns*$^{-/-}$ mice (**Table 1**).

Correlations between transduction efficiencies in blood and transduced bone marrow-derived cells present in tissues

Reverse transcription-quantitative PCR (qPCR) of total RNA purified from whole blood of pCCL-CTNS–transplanted *Ctns*$^{-/-}$ mice with CTNS-specific primers showed that *CTNS* transcripts were expressed in circulating blood cells; the mean value was 332 ± 238 expressed as 18S-normalized fold change (*CTNS* expression level was 199 ± 149 in normal human blood; $n = 3$). We then performed qPCR on genomic DNA from the tissues and blood of 18 pCCL-CTNS–transplanted *Ctns*$^{-/-}$ mice with LV-specific primers. No lentiviral DNA was detected in the control *Ctns*$^{-/-}$ mice. The pCCL levels measured in the transplanted *Ctns*$^{-/-}$ mice were as follows and

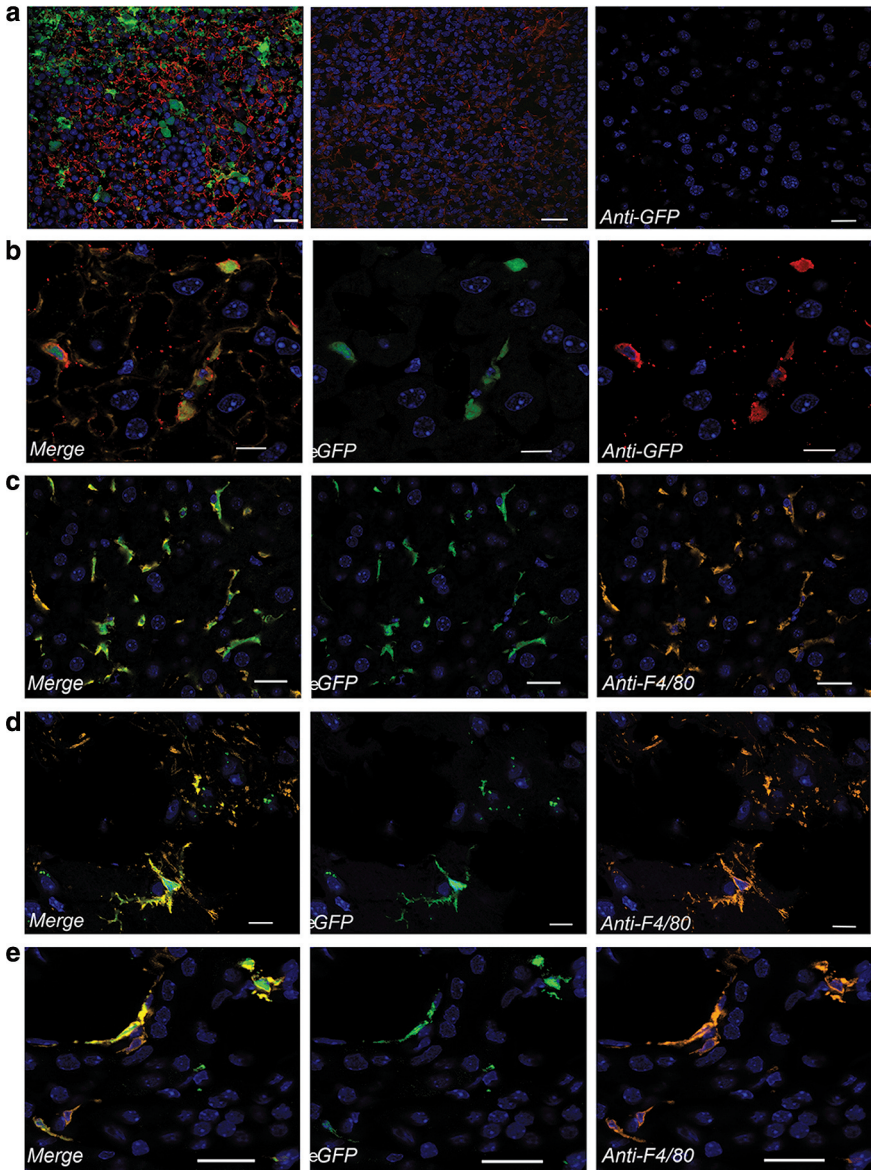

Figure 2 Tissue integration of *ex vivo* transduced bone marrow-derived cells after transplantation. Representative confocal microscopy pictures of tissue sections from *Ctns*$^{-/-}$ mice transplanted with pCCL-eGFP–transduced HSPC (n = 8) and controls. Nuclei are stained by DAPI (blue) and direct eGFP fluorescence is seen in green. (**a**) Representative sections of the spleen of mice transplanted with pCCL-eGFP–transduced HSPC (left picture) compared with non-transplanted control (middle picture) show abundant eGFP-expressing cells exclusively in the transplanted mice. F-actin intermediate filament staining by Bodipy-Phalloidin showing tissue structure is seen in red. In the right picture, the immunostaining for eGFP (red channel) of liver from non-transplanted control did not show any unspecific staining. (**b**) Representative sections of liver from mice transplanted with pCCL-eGFP–transduced HSPC immunostained with an anti-GFP antibody (seen in red). eGFP expressing bone marrow-derived eGFP-expressing cells colocalize with the anti-GFP immunostaining, proving the specificity of the green fluorescence. F-actin intermediate filament staining by Alexa Fluor 647-Phalloidin is seen in orange in the merge picture. (**c**–**e**) Immunostaining for F4/80. Representative sections of *Ctns*$^{-/-}$ mice transplanted with pCCL-eGFP–transduced HSPC show eGFP expressing bone marrow-derived cells coexpressing F4/80 in the (**c**) liver, (**d**) the brain, and the (**e**) kidney demonstrating their differentiation into Kupffer cells, microglial cells, and inflammatory dendritic cells, respectively. Bars: 20 µm (in **a**,**c**,**e**); 10 µm (**b**,**d**). DAPI, 4′,6-diamidino-2-phenylindole; eGFP, enhanced green fluorescent protein; HSPC, hematopoietic stem and progenitor cell.

correspond to the copy of viral vector per cell present in the corresponding compartment: blood, 1.573 ± 1.868; brain, 0.001 ± 0.0005; kidney, 0.0363 ± 0.0284; liver, 0.066 ± 0.047; spleen, 0.273 ± 0.161. In order to determine whether LV quantity could be easily predicted in tissues, we performed linear regression analyses between pCCL levels in the different tissues as a function of blood pCCL levels. We found significant correlations for all the tissues tested except the kidney, showing that the higher the level of LV DNA detected in the blood, the higher the levels are in the tissues: brain, $F_{1,15} = 5.9504$, $P = 0.0286$, $R^2 = 0.298258$; kidney, $F_{1,17} = 0.3529$, $P = 0.5608$, $R^2 = 0.021578$; liver, $F_{1,16} = 6.3528$, $P = 0.0235$, $R^2 = 0.297514$; spleen, $F_{1,16} = 5.8394$, $P = 0.0289$, $R^2 = 0.280209$.

We did not observe any cases of tumors, leukemia or unexpected toxicity in any of the transplanted mice with LV-transduced HSPC for up to 12 months follow-up (n = 36). Basic tissue histology of brain, kidney, and muscle was performed on all the mice

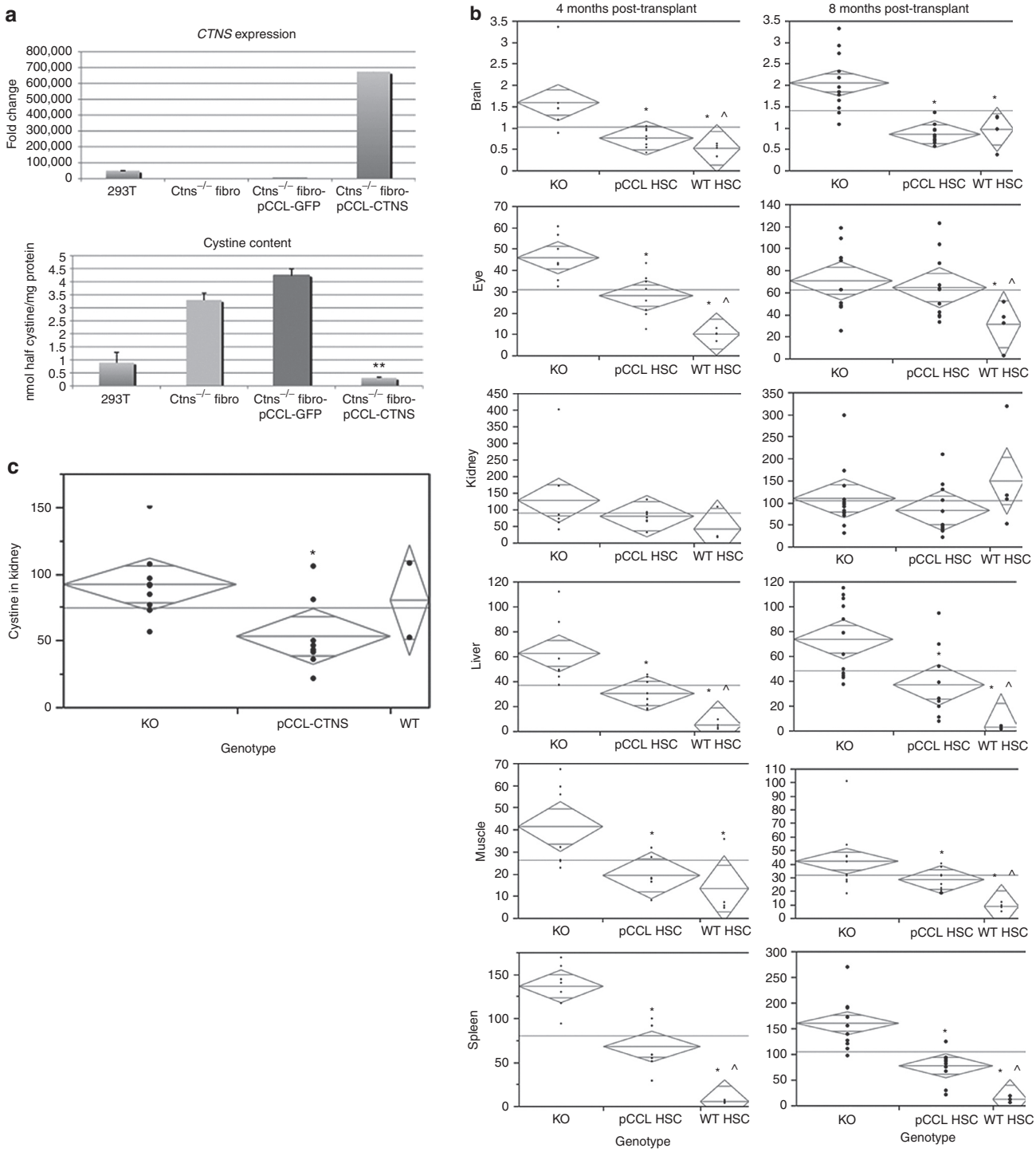

Figure 3 Effect of pCCL-CTNS in cystine content levels *in vitro* and *in vivo*. (**a**) The upper panel shows the expression levels of the human *CTNS* transgene in pCCL-CTNS–transduced Ctns$^{-/-}$ fibroblasts compared with pCCL-eGFP–transduced and control Ctns$^{-/-}$ fibroblasts as negative controls, and 293T, which are human cells, as positive control. The lower panel shows that cystine content is significantly reduced in pCCL-CTNS–transduced Ctns$^{-/-}$ fibroblasts compared with both pCCL-eGFP–transduced and control Ctns$^{-/-}$ fibroblasts. $^{**}P < 0.0001$. (**b**) Cystine content levels (nmol half cystine/mg protein) in *Ctns*$^{-/-}$ mice (males and females) transplanted with either pCCL-CTNS–transduced Ctns$^{-/-}$ HSPC (pCCL HSC) or WT congenic HSPC (WT HSC) compared to control non-treated *Ctns*$^{-/-}$ mice (KO) at 4 and 8 months post-transplant in the different tissues tested. Each point represents individual data from each mouse and the mean value is represented by the median line of the diamonds; the extremities of the diamonds represent the 95% confidence intervals in each group. Significant decrease in cystine levels is observed in pCCL-CTNS–treated mice in the majority of tissues compared with control *Ctns*$^{-/-}$ mice. $^{*}P < 0.05$ compared with non-treated *Ctns*$^{-/-}$ mice, $^{\wedge}P < 0.05$ compared with pCCL-CTNS–treated *Ctns*$^{-/-}$ mice. (**c**) Kidney cystine content (nmol half cystine/mg protein) in non-treated male *Ctns*$^{-/-}$ mice (KO), transplanted with pCCL-CTNS–transduced Ctns$^{-/-}$ HSPC (pCCL HSC) or with WT congenic HSPC (WT HSC) at 8 months post-transplant. $^{*}P < 0.05$ compared with non-treated *Ctns*$^{-/-}$ mice. GFP, green fluorescent protein; HSC, hematopoietic stem cell; KO, knockout; WT, wild-type.

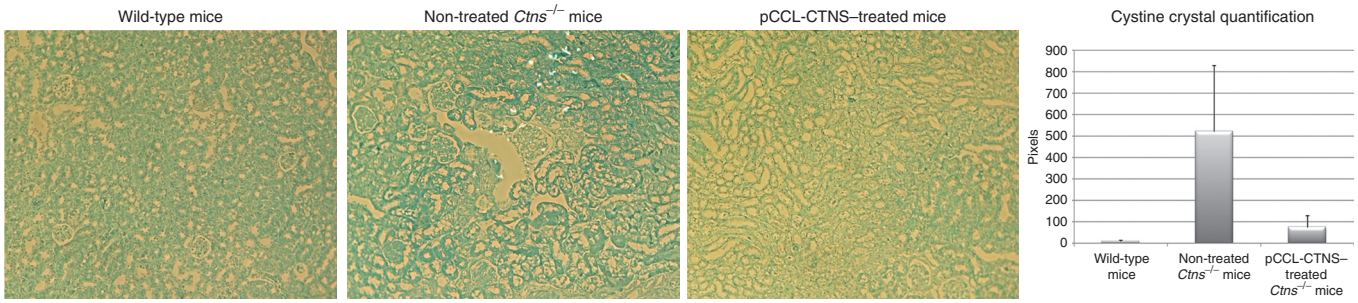

Figure 4 Cystine crystal quantification in kidney sections from male *Ctns*$^{-/-}$ mice. Kidney sections stained with methylene blue in ethanol were used to observe cystine crystals. Low magnification pictures were analyzed using ImageJ software. Abundant cystine crystals were observed in kidney sections from non-treated *Ctns*$^{-/-}$ males ($n = 9$) in contrast to pCCL-CTNS–treated males ($n = 8$). Wild-type mice ($n = 4$) were used as negative control for our method of cystine crystal detection using ImageJ. Error bars are defined as mean ± SD, *$P < 0.05$.

Table 1 Serum and urine analyses for renal function of 9–11 months old males

	Wild-type, $n = 6$	Control Ctns$^{-/-}$, $n = 9$	pCCL-CTNS–treated Ctns$^{-/-}$, $n = 8$
Serum			
Creatinine (mg/dl)	0.27 ± 0.03	0.31 ± 0.08	0.22 ± 0.11[a]
Creatinine clearance (ml/minute/kg)	4.44 ± 0.39	3.86 ± 1.42	4.89 ± 5.56
Urea (mg/dl)	14.55 ± 1.87	28.29 ± 16.11[b]	24.10 ± 7.32[b]
Phosphate (mg/dl)	12.25 ± 2.38	13.20 ± 2.90	13.16 ± 2.21
Urine			
Phosphate (mmol/24 hours)	6.82 ± 2.90	8.84 ± 4.60	4.78 ± 3.87[a]
Volume (ml)	1.05 ± 0.51	1.26 ± 0.54	0.70 ± 0.60[a]

[a]$P < 0.05$ compared with Ctns$^{-/-}$. [b]$P < 0.05$ compared with wild-type mice.

transplanted with pCCL-CTNS ($n = 20$) and did not reveal any abnormalities.

Chromosomal insertion sites were analyzed by ligation-mediated PCR in the spleen and blood of 13 pCCL-CTNS–transplanted mice. **Figure 5** reveals the finding of two distinct adjacent amplicons that could suggest the presence of a clonal pattern. However, sequencing of these two bands revealed that both amplicons were located in noncoding genomic DNA in chromosome 10 and 16, implying that no insertional mutagenesis occurred.

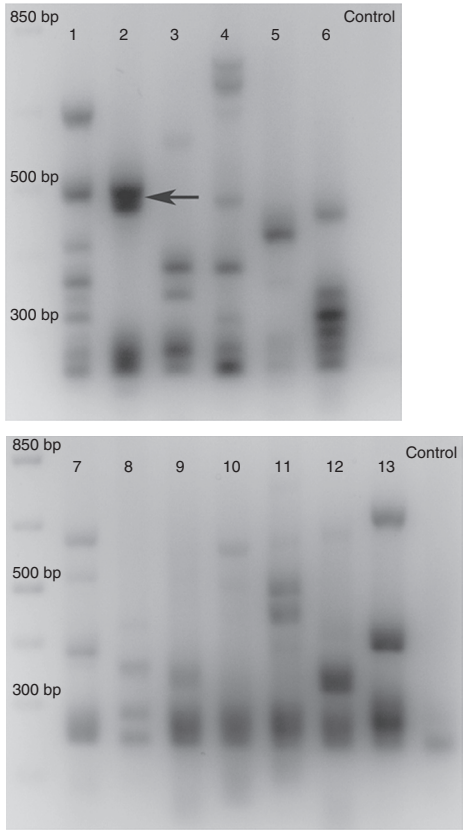

Figure 5 LM-PCR analysis of the *Ctns*$^{-/-}$ mice transplanted with pCCL-CTNS–transduced HSC. Two gels are depicted, the first line of each gel is the ladder and the last lane represents a non-transplanted mouse control. Each lane shows the amplicons corresponding to the distribution of the lentiviral vector insertion sites obtained by LM-PCR in the spleen of each mouse tested (#1–13). Two dominant amplicons (arrow) were observed in one of the transplanted mice (#2). HSC, hematopoietic stem cell; LM-PCR, ligation-mediated PCR.

Cross-correction may occur in cystinosis

To study a potential transfer of the functional cystinosin from bone marrow-derived cells to host adjacent cells, we generated a new Ctns$^{-/-}$ mouse model, the DsRed *Ctns*$^{-/-}$ mice, that constitutively express the DsRed reporter gene. This new mouse model was used to isolate HSPC that were DsRed Ctns$^{-/-}$. We also generated a pCCL LV expressing a cystinosin-eGFP fusion protein. The functionality of the fusion protein was verified *in vitro* by transducing Ctns$^{-/-}$ fibroblasts. Cystinosin-eGFP fusion protein appeared in intracellular vesicles that colocalized with a lysosome-staining dye, LysoTracker, demonstrating that cystinosin is targeted correctly to the lysosomes (**Figure 6a**). Western blot analysis with an anti-GFP antibody revealed several bands between 70 and 85 kDa in the transduced fibroblasts that correspond to the cystinosin-eGFP at different stages of glycosylation[10] (**Figure 6b**). Finally, cystine content was significantly decreased in the pCCL-CTNSeGFP–transduced Ctns$^{-/-}$ fibroblasts ($n = 6$) compared with non-transduced controls ($n = 6$) proving that the protein was functional (**Figure 6c**).

To investigate a potential cross-correction *in vitro*, we cocultured DsRed Ctns$^{-/-}$ fibroblasts and pCCL-CTNSeGFP–transduced Ctns$^{-/-}$ fibroblasts for 2 weeks. Microscopy analysis revealed the

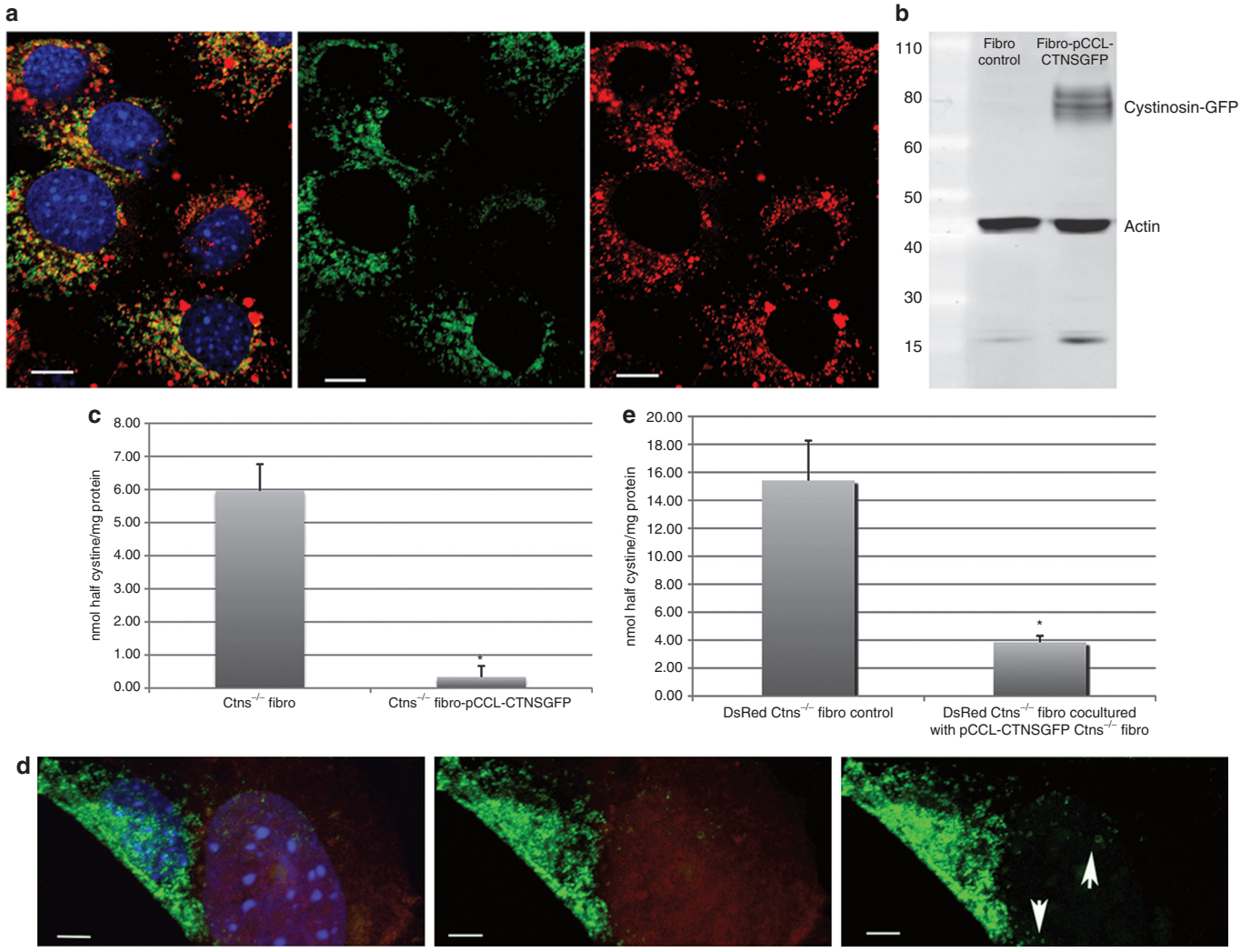

Figure 6 ***In vitro*** **study of cross-correction.** Ctns$^{-/-}$ fibroblasts were stably transduced by a lentivrial vector driving the expression of the fusion protein cystinosin-eGFP (pCCL-CTNSeGFP). (**a**–**c**) Demonstration of the functionality of the fusion protein. (**a**) Cystinosin-eGFP seen in green is targeted to the lysosomes, colocalizing with the LysoTracker staining seen in red. Bar: 10 µm. (**b**) Western blot analysis with an anti-GFP antibody revealed bands between 70 and 85 kb in the pCCL-CTNSeGFP–transduced fibroblasts. (**c**) Cystine measurements showed a significant cystine decrease in the CTNSeGFP-expressing fibroblasts compared with Ctns$^{-/-}$ fibroblast controls. *$P < 0.0001$. (**d**,**e**) Demonstration of the cross correction *in vitro* by coculture of pCCL-CTNSeGFP–transduced fibroblasts and DsRed Ctns$^{-/-}$ fibroblasts seen in red. (**d**) Green vesicles can be seen in the DsRed-expressing fibroblasts, demonstrating the transfer of cystinosin. Bar: 5 µm. (**e**) Cystine content was significantly decreased in the sorted DsRed-expressing cells cocultured pCCL-CTNSeGFP compared with the sorted DsRed-expressing cells cultured alone. Error bars are defined as mean ± SD. *$P < 0.0001$. eGFP, enhanced green fluorescent protein.

presence of green vesicles in the DsRed cells, suggesting the transfer of the cystinosin from the CTNS-expressing cells to adjacent cells (**Figure 6d**). Cystine measurements of the DsRed-expressing cells after sorting to exclude the pCCL-CTNSeGFP-fibroblasts showed a significant cystine decrease in the cocultured DsRed Ctns$^{-/-}$ fibroblasts compared with the sorted DsRed Ctns$^{-/-}$ cells cultured alone (**Figure 6e**). These data showed that a transfer of functional cystinosin occurs *in vitro* from CTNS-expressing cells to adjacent cells.

To study potential cross-correction *in vivo*, we transplanted our original Ctns$^{-/-}$ mouse model with DsRed Ctns$^{-/-}$ HSPC transduced with pCCL-CTNSeGFP (CTNSeGFP-DsRed-HSPC mice; $n = 5$). We used non-transplanted ($n = 2$) and DsRed Ctns$^{-/-}$ HSPC-transplanted (DsRed-HSPC mice; $n = 2$) *Ctns*$^{-/-}$ mice as controls. DsRed-expressing donor cell blood engraftment was 96.4 ± 1.1% in DsRed-HSPC mice and 81.3 ± 9.1% in the CTNSeGFP-DsRed-HSPC mice. In both groups of mice, bone marrow-derived DsRed-expressing cells were observed abundantly in tissues by confocal microscopy as expected; we focused our studies on the liver (**Figure 7**). However, only in CTNSeGFP-DsRed-HSPC mice could we observe eGFP-positive intracellular vesicles in some DsRed-expressing bone marrow-derived cells within tissues (**Figure 7**). The eGFP-positive intracellular vesicles colocalized with the lysosome-specific antibody Lamp-2, showing that cystinosin was targeted to the lysosomes (**Figure 7b**). Some of the eGFP-positive intracellular vesicles in CTNS-expressing DsRed cells were large structures (**Figure 7a,b**). Remarkably, we also observed non-color host tissue cells containing discrete green

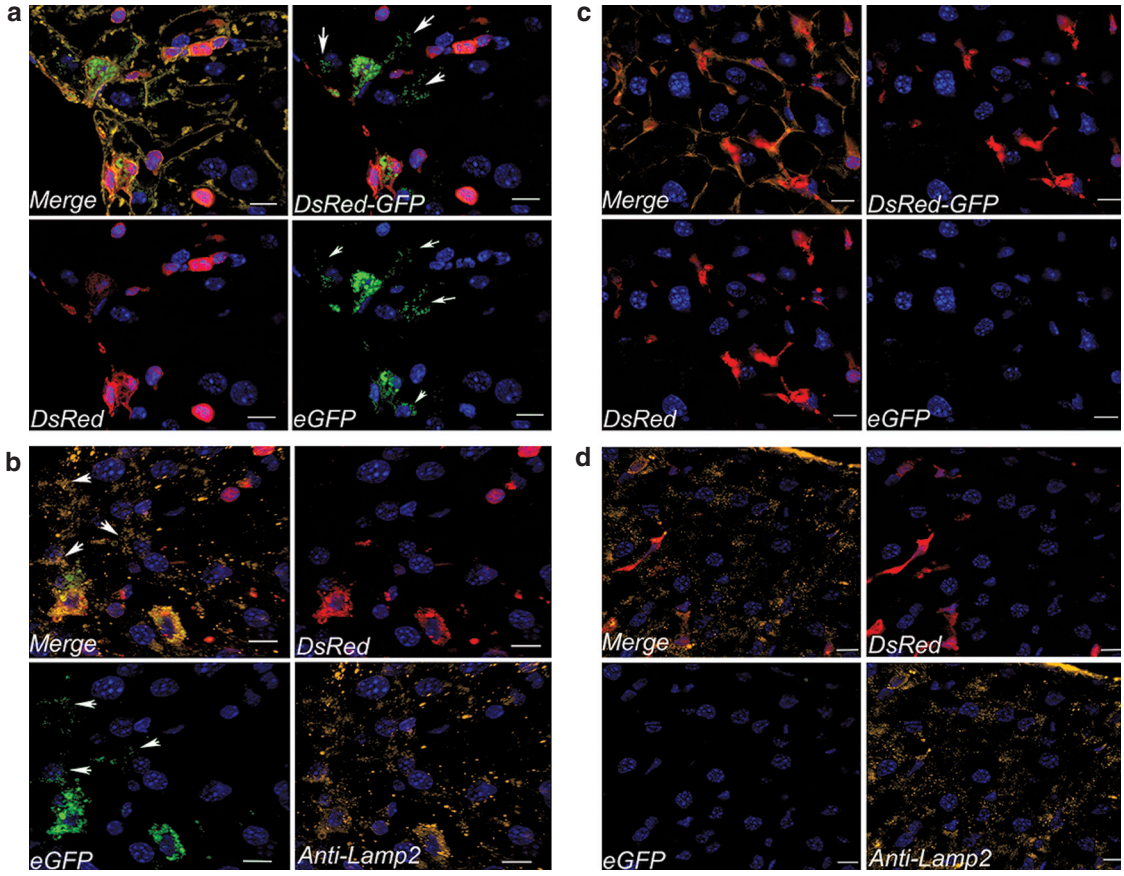

Figure 7 ***In vivo*** **transfer of cystinosin from CTNS-expressing bone marrow-derived cells to Ctns-deficient host cells.** Representative confocal microscopy pictures of liver sections from (**a**,**b**) *Ctns*$^{-/-}$ mice transplanted with pCCL-CTNSeGFP–transduced DsRed Ctns$^{-/-}$ HSPC (n = 5) and (**c**,**d**) *Ctns*$^{-/-}$ mice transplanted with non-transduced DsRed Ctns$^{-/-}$ HSPC as controls (n = 2). Nuclei are stained by DAPI (blue), DsRed-expressing bone marrow-derived cells are seen in red and cystinosin-eGFP fusion proteins are seen in green. Green intracellular vesicles are observed exclusively in *Ctns*$^{-/-}$ mice transplanted with pCCL-CTNSeGFP–transduced DsRed Ctns$^{-/-}$ HSPC (as shown in **a**,**b**). Large eGFP-positive vesicular structures are observed in DsRed-expressing bone marrow-derived cells but also discrete green vesicles can be seen in the host cells, demonstrating a transfer of the cystinosin from CTNS-expressing cells to the adjacent host cells (arrows in **a**,**b**). (**a**,**c**) F-actin intermediate filament staining by Alexa Fluor 647-Phalloidin is seen in orange and shows the cell boundaries. (**b**,**d**) Immunostaining with the lysosomal marker LAMP-2 is seen in orange. eGFP-positive vesicles observed in both DsRed-expressing cells and host cells colocalize with the anti-LAMP-2 staining (as shown in **b**). Bars: 10 µm. DAPI, 4′,6-diamidino-2-phenylindole; eGFP, enhanced green fluorescent protein.

vesicles consistent with the transfer of cystinosin-eGFP fusion protein from the transduced bone marrow-derived DsRed cells (**Figure 7a**; arrows). These vesicles also colocalized with anti-Lamp 2 antibodies (**Figure 7b**; arrows) demonstrating that the cystinosin-eGFP fusion protein was located in the correct intracellular compartment. No eGFP-positive intracellular vesicles were observed in the control DsRed-HSPC mice (**Figure 7c,d**).

DISCUSSION

We previously showed the potential of using wild-type HSPC transplantation for cystinosis, a multisystemic LSD due to a dysfunctional lysosomal transmembrane protein.[17] These results indicated that bone marrow cell transplantation could be a long-term systemic treatment for this disease, but also for other multisystemic diseases due to dysfunctional intracellular proteins. However, the risks related to allogeneic HSC transplantation limit its implementation especially when a treatment delaying the progression of the disease exists as in the case of cystinosis. Autologous transplantation of genetically modified HSPC would minimize the risks and thus would generalize the use of such therapy for genetic diseases. However, gene therapy also carries some risks as demonstrated by several cases of leukemia in a clinical trial using murine leukemia virus-transduced human HSC for X-linked severe combined immunodeficiency children.[32] In contrast to murine leukemia virus vectors, SIN-LV may be safer virus vectors for gene therapy.[23,25]

We showed that *ex vivo* lentiviral-transduced Ctns$^{-/-}$ HSPC expressing a functional *CTNS* gene led to long-term cystine decreases in all tissues. In contrast, a previous study using a human adenovirus vector containing *CTNS* administered *via* tail vein in the *Ctns*$^{-/-}$ mice showed only a short-term impact on cystine decrease in the liver.[33] The variation of results in cystine levels we obtained probably depends on the transduction efficiency of the transplanted HSPC and variations in engraftment levels as previously described.[18] We measured the transduction efficiency in the peripheral blood and showed that this was significantly correlated to the quantity of corrected cells present in tissues. We propose that this strategy may become a noninvasive method to monitor future cystinotic patients after transplantation. Moreover, we showed

previously that the level of Ctns-expressing donor-derived blood cell engraftment was a determinant factor for kidney preservation in the *Ctns*$^{-/-}$ mice after syngeneic HSPC transplantation.[18]

Curiously, the kidney was the only tissue in which no significant cystine decrease could be obtained with either wild-type or lentiviral-modified HSPC. In the process of understanding the nature of this discrepancy, we discovered that a significant difference exists in kidney cystine content between male and female *Ctns*$^{-/-}$ mice. Is that true in humans? Why is there a difference in cystine content between males and females in the kidney and not the other organs? These questions will need further investigation and highlight the complexity of kidney pathogenesis in cystinosis. In this study, when we analyzed the males separately at 8 months post-transplantation, cystine content and cystine crystals were significantly decreased in the kidney of pCCL-CTNS–treated mice compared with non-treated controls and the renal function was improved. These data show the beneficial therapeutic effect of the transplantation of genetically modified Ctns-deficient HSPC using a LV to introduce a functional *CTNS* gene in the *Ctns*$^{-/-}$ mice.

We showed that lentivirus-transduced HSPC retained the same differentiative capacity after transplantation as wild-type HSPC, capable of migrating abundantly to all tissues in *Ctns*$^{-/-}$ mice and engraft as shown previously.[17] This is an important point as the *ex vivo* cytokine activation of HSPC to facilitate transduction may alter the lineage commitment pathways of progenitor cells.[34,35] We observed differentiation into dendritic cells in the kidney or resident macrophage-derived cells within tissues such as Kupffer cells in the liver and microglial cells in the brain. In most tissues, the impact of transplanting wild-type HSPC was greater than pCCL-CTNS–transduced HSPC. These data suggest that the quantity of progenitors expressing *CTNS* matters more than the overexpression of *CTNS* per cell. We suspect that resident macrophage-derived cells have a major role in the pathogenesis of cystinosis. Their replacement by bone marrow-derived cells expressing *CTNS* could explain the majority of cystine depletion by the phagocytosis of cystine-overloaded cells. Indeed, Kupffer cells contain 75% of the total cystine content in the liver whereas they only represent ≤10% of the total cells in the liver.[33]

However, we showed previously a short-term improvement after mesenchymal stem cell transplantation in *Ctns*$^{-/-}$ mice including tissue cystine decrease and renal function amelioration, suggesting a paracrine effect of the mesenchymal stem cells.[17] Also, in the brain, lentiviral-transduced cells had a higher and more consistent impact on cystine decrease than the wild-type HSPC at 8 months post-transplantation. This phenomenon has been previously described in the case of HSC gene therapy for the treatment of the central nervous system anomalies in the murine model of metachromatic leukodystrophy.[27] The hypothesis that was proposed was overexpression of the aryl-sulfatase A gene in bone marrow-derived microglial cells delivered functional enzymes to the adjacent cells in the brain. Thus, all these data suggest that a transfer of the cystinosin protein to adjacent cells could occur. Cross-correction has been well demonstrated in the case of secreted enzymes in several LSDs such as Hurler syndrome.[36] In this case and in the case of other LSDs due to a lysosomal enzyme deficiency, the uptake of the enzymes from the extracellular milieu by neighboring cells is performed *via* the mannose-6-phosphate receptor that subsequently mediates endocytosis and lysosomal targeting.[37–39] In the case of cystinosis, the protein involved is a seven transmembrane lysosomal protein. Direct secretion of the cystinosin is not possible, but cross-correction could occur *via* transfer of vesicles containing cystinosin.

To test this hypothesis, we generated a new cystinosis mouse model that ubiquitously expressed the DsRed reporter gene. DsRed Ctns$^{-/-}$ HSPC were transduced with a LV containing the CTNS-eGFP fusion cDNA and transplanted in our regular *Ctns*$^{-/-}$ mice. Cystinosin-eGFP was observed in the lysosomes of DsRed-expressing bone marrow-derived cells within the tissues. Some of the Lamp-2-positive eGFP-positive vesicles looked like large structures, probably due to the clustering and/or fusion of lysosomes as a consequence of *CTNS* overexpression as previously described.[10] The long-term consequence of this phenomenon is unknown. Remarkably, we also observed host cells containing discrete eGFP-positive intracellular vesicles. This showed that, even if cystinosin is a lysosomal transmembrane protein, a transfer to adjacent cells is possible. *In vitro*, we showed that cystinosin transfer led to cystine decrease in Ctns-deficient cells. The transfer could occur *via* CTNS genetic material-containing microvesicles or exosomes, both released from the endosomal compartment.[40,41] We showed that cystinosin is present in lysosomal vesicles after transfer but we do not know whether CTNS mRNA or cystinosin protein were transferred. Most of the microvesicles/exosomes described contain microRNA or mRNA[41] but proteins have also been found.[42] Further studies will be necessary to answer this question. The second question will be to determine the route of transfer. Are membrane vesicles shed from cells to mediate transfer of CTNS genetic material to adjacent cells? Alternatively, are intercellular plasma membrane connections such as nanotubes involved?[43] Bone marrow stem cells have previously been shown to have a paracrine effect *via* microvesicle exchange for tissue repair.[44,45] Nanotubes between macrophages have been described and were shown to allow the trafficking of mitochondria and intracellular vesicles such as lysosomes.[46] In our case, direct transfer of cystinosin-containing lysosomes could be possible. We believe that bone marrow-derived macrophages within tissues expressing a functional *CTNS* gene could have a double therapeutic action by phagocytosing cystine-overloaded cells and by providing a functional protein to adjacent cells.

This work represents the first step towards a clinical trial for cystinosis using autologous HSPC genetically modified *ex vivo* to express a functional *CTNS* transgene using a SIN-LV. We were also able to provide some insights into the mechanism of the long-term therapeutic effect of transplanted HSPC expressing a functional *CTNS* and showed the possibility of cross-correction in the case of cystinosis treated by transplantation of gene-modified HSPC. This is a proof-of-concept for many hereditary genetic diseases for which curative therapy requires the addition of the gene to many cells, typically in multiple tissue compartments, and where the protein involved is an intracellular transmembrane protein.

MATERIALS AND METHODS

Mice. C57BL/6 *Ctns*$^{-/-}$ mice were provided by Dr Antignac (Inserm U983, Paris, France). B6.Cg-Tg(CAG-DsRed*MST)1Nagy/J (Jackson Laboratory, Bar Harbor, ME) mice were cross-bred with the C57BL/6 *Ctns*$^{-/-}$ mice to produce the transgenic DsRed *Ctns*$^{-/-}$ mice constitutively expressing the

DsRed fluorescent protein under the control of the chicken β-actin promoter coupled with the cytomegalovirus immediate early enhancer. All strains were bred continuously at The Scripps Research Institute (TSRI) such as wild-type C57BL/6 mice. All protocols were approved by the AAALAC-Accredited Institutional Animal Care and Use Committee of TSRI.

Generation of CTNS-, eGFP-, and LUC-LVs. The SIN-LV, pCCL-EFS-X-WPRE (pCCL) was used for gene transfer. The vector backbone is based on the pCCL LVs[47] and contains the intron-less human elongation factor 1α promoter (242 bp) to drive the transgene expression.[48] The *eGFP*, *LUC*, and the human *CTNS* cDNA as well as the fusion *CTNS-eGFP* cDNA were inserted into pCCL at the *Bam*HI and *Sal*I restriction sites; they were named pCCL-eGFP, pCCL-LUC, pCCL-CTNS, and pCCL-CTNSeGFP, respectively. *CTNS* was amplified from the vector pcDNA-CTNS kindly provided by Dr Antignac.

Production of LV and titers. Infectious lentiviral particles were produced using the transient tri-transfection procedure in human embryonic kidney 293T cells. Packaging plasmids (pMDLg/pRRE, pHCMV-G, and pRSV-Rev) along with the expression constructs, were used resulting in the assembly of vesicular stomatitis virus-G glycoprotein pseudotyped viral particles. Vector particles were collected in 25 ml of Stemspan medium (StemCell Technologies, Vancouver, British Columbia, Canada) and concentrated 100 times by ultracentrifugation at 25,000 rpm for 2 hours at 4 °C. Titers of concentrated virus were measured by infection of 293T cells after serial dilutions of the virus preparations and determined by flow cytometry for pCCL-eGFP and IVIS imaging system for pCCL-LUC. Titers for pCCL-CTNS viral particles were measured by infection of $Ctns^{-/-}$ fibroblast cells and determined by qPCR on genomic DNA as described below. Viral titers of concentrated supernatant ranged from 6×10^8 to 8×10^8 transducing units/ml depending on the vector. Replication competent lentivirus was absent in the vector preparation and the blood of the transplanted mice using a vector rescue assay.

HSPC enrichment, transduction, and transplantation. Bone marrow cells were flushed from the femur and tibia of 6–8 weeks old *Ctns*$^{-/-}$ or wild-type mice. HSPC were isolated by immunomagnetic separation using anti-Sca1 antibody conjugated to magnetic beads (Miltenyi Biotec, Auburn, CA). $Sca1^+$ HSPC were resuspended in Stemspan supplemented with murine stem cell factor, thrombopoietin, and murine FMS-like tyrosine kinase 3-ligand (mFlt3L) at a concentration of 100 ng/ml, and murine interleukin-6 (mIL-6; PeproTech, Rocky Hill, NJ) at 20 ng/ml. The cells were plated at a density of 2×10^6 cells in 0.5 ml of media per well in a 24-well plate. The plate was pretreated with 300 µl of RetroNectin (Takara Bio USA, Madison, WI) at 20 µg/ml. $Sca1^+$ HSPC were transduced with lentiviral particles in the presence of polybrene (4 µg/ml) and incubated for 16 hours at 37 °C, 5% CO_2. Cells from each well were collected and washed twice in phosphate-buffered saline and then resuspended in 200 µl of phosphate-buffered saline. Tail vein injection of 100 µl containing ~1×10^6 cells was performed in each *Ctns*$^{-/-}$ mice lethally irradiated (8Gy) on the previous day.

Lineage reconstitution determination with transduced HSPC. Fresh blood of pCCL-eGFP-HSPC–transplanted mice was treated with red blood cell lysis buffer (eBioscience, San Diego, CA) and analyzed by flow cytometry to quantify $eGFP^+$ cells and hematopoietic lineage-specific cell types after subset antibody staining. T cells were stained with phycoerythrin-conjugated anti-CD3ε, B cells with phycoerythrin-conjugated anti-CD19, and macrophages with phycoerythrin-conjugated anti-CD11b (BD Biosciences, San Jose, CA). Appropriate isotype controls were used for each.

Immunofluorescence analysis. Tissues were fixed in formaldehyde 5%, equilibrated in sucrose 20% overnight and frozen in Tissue-Tek Optimal Cutting Temperature buffer at −80 °C (Sakura Finetek U.S.A, Torrance, CA); 10 µm sections were cut and stained with DAPI, Bodipy-Phalloidin or Alexa Fluor 647-Phalloidin (1:500 dilutions for 30 minutes; Molecular Probes, Eugene, OR). Tissues were also stained with a rabbit anti-GFP antibody (1:200 dilution; Abcam, Cambridge, MA) and a rabbit anti-LAMP2 antibody (1:100 dilution; Abcam), followed by a donkey anti-rabbit conjugated with Cy5 (dilution 1:200; Jackson ImmunoResearch Laboratories, West Grove, PA). Tissues were also stained with a directly labeled Alexa Fluor 647-rat anti-mouse F4/80 antibody (1:25 dilution; AbD Serotec, Raleigh, NC). Culture cells were stained with a LysoTracker-Red DND-99 (Invitrogen, Carlsbad, CA) at a concentration of 75 nmol/l for 1 hour before fixation. Images were acquired using a Zeiss LSM 710 laser scanning confocal microscope attached to a Zeiss Observer Z_1 (BioRad-Carl Zeiss, Thornwood, NY). All images were 8-bit optical image slices (0.5 µm interval step slices) acquired using LaserSharp 2000 software (BioRad, Hercules, CA). Images were then analyzed with IMARIS 4.2 imaging software (Bitplane Scientific Solutions, Saint Paul, MN) to generate 3-D reconstruction series of optical slices (Z-stacks).

Live animal LUC imaging. Mice transplanted with pCCL-LUC–transduced HSPC were analyzed using the IVIS Imaging System 200 Series (Caliper Life Sciences, Hopkinton, MA) as previously described.[17]

Histology. Kidneys were fixed in formalin and embedded in paraffin. Sections were briefly stained with methylene blue in absolute alcohol for the detection of cystine crystals. Cystine crystals were quantified using ImageJ software (NIH, Bethesda, MD) on low magnification pictures of methylene blue stained sections covering most of the kidney section for each mouse. The threshold was adjusted to recognize specifically the cystine crystals, and pixels were quantified.

Cystine content measurement. Explanted tissues were ground in 750 µl of N-ethylmaleimide (Fluka Biochemika, Bushs, Switzerland) at 650 µg/ml using the Precellys 24 homoginizer (Bertin Technologies, Montigny-le-Bretonneux, France). For the *in vitro* assays, sorted cells were resuspended in 150 µl N-ethylmaleimide and sonicated for 10 seconds at an amplitude of 2 on ice. Proteins were precipitated using 15% 5-sulfosalicylic acid dihydrate (Fluka Biochemika, Buchs, Switzerland), resuspended in NaOH 0.1 N and measured using the Pierce BCA protein assay kit (Pierce, Rockford, IL). The cystine-containing supernatants were sent to the UCSD Biochemical Genetics laboratory for measurement by mass spectrometry as described previously.[18]

Blood and urine analysis. Serum was obtained by eye bleeds or cardiac puncture, and 24-hour urine collections were done in metabolic cages. Serum and urine phosphate levels, and serum creatinine and urea were estimated by using colorimetric assays according to the manufacturer recommendations (BioAssay Systems, Hayward, CA).

Blood and tissue DNA and RNA extraction. Tissue DNA and RNA were isolated from explanted tissues using the Qiagen AllPrep DNA/RNA Mini kit (Qiagen, Valencia, CA) and Qiagen QIAcube after homogenization in Precellys 24. Blood RNA was purified using the RNeasy Protect Animal Blood Kit (Qiagen). Blood DNA was purified with the DNeasy Tissue Kit (Qiagen) using the animal blood protocol.

Reverse transcription and qPCR. One microgram of blood RNA was reverse transcribed using iScript cDNA Synthesis Kit (Bio-Rad, Hercules, CA). qPCR were performed using either 2 µl of cDNA or 200 ng of genomic DNA and 2x Universal TAQ man master mix (Applied Biosystems, Foster City, CA) on an Applied Biosystems 7900 HT (Applied Biosystems). Primers and probes were obtained from Applied Biosystems:

- *CTNS*-specific primers were designed in exon 9: *Ctns* oligo 1: CAAATACCCCAACGGAGTGAA, *CTNS* oligo 2: GCGTGCAGGCTGAAGAAGAC, and *CTNS* probe: CCCGTGAACAGCAAC.
- Lentivirus-specific primers were designed in the HIV-1 Psi region: pCCL oligo 1: ACTTGAAAGCGAAAGGGAAAC, pCCL oligo 2: CGCACCCATCTCTCTCCTTCT, and pCCL probe: AGCTCTCTCGACGCAGGACTCGGC.

To construct a standard curve, DNA extracted from the clonal population of HT29 cells (colorectal adenocarcinoma) containing two proviral copies of SMPU-MND-huADA[49] was serially diluted into DNA extracted from untransduced HT29 cells. qPCR were performed on the serial dilutions and DNA extracted from blood and tissues, and the ΔCt were obtained from normalized values against an endogenous control (18S). To determine the vector copy per cell, values were determined from the standard curve.

Ligation-mediated PCR. Lentiviral integration site patterns were detected on genomic DNA from blood and spleen as previously described.[50] Briefly, genomic DNA was restriction digest by Tsp509I enzyme (New England Biolabs, Ipswich, MA), precipitated and preamplified by primer extension using an long terminal repeat (LTR) vector-specific 5′-biotinylated primer pCCL LTR 1F (5′-GAGCTCTCTGGCTAACTAGG-3′) and pfu DNA polymerase (Stratagene, Cedar Creek, TX). Biotylated extension products were cleaned-up using QIA Quick PCR kit (Qiagen) and selected using 200 µg of Dynabeads M-280 Streptavidin (Invitrogen). Asymmetric polylinker (Linker-oligo 1: 5′-GACCCGGGAGATCTGAATTCAGTGGCACAGCAGTTAGG-3′; Linker-oligo 2: 5′-CCTAACTGCTGTGCCACTGAATTCAGATCTCCCG-3′; 40 µmol/l) were ligated to the vector-specific extension products using the Rapid DNA Ligation kit (Roche Diagnostics, Indianapolis, IN). The products were amplified by a first PCR and nested PCR with the Extensor HI-Fidelity PCR master mix (ABgene, Hamburg, Germany) using a LTR vector-specific primer and a linker-specific primer as followed:

- First PCR: pCCL LTR 2F (5′-GAACCCACTGCTTAAGCCTCA-3′) and OC1 (5′-GACCCGGGAGATCTGAATTC-3′)
- Nested PCR: pCCL LTR 3F (5′-AGCTTGCCTTGAGTGCTTCA-3′) and OC2 (5′-AGTGGCACAGCAGTTAGG-3′).

PCR products were visualized on a 2% agarose gel. Predominant bands were cut from the gel, cleaned-up using MinElute kit (Qiagen) and cloned into pCR-Blunt II-TOPO TA Cloning kit (Invitrogen). Sequencing of the insert was performed using TOPO-specific primer.

Western blot analysis. Cells were homogenized in RIPA lysis buffer (Sigma, St Louis, MO) containing protease and phosphatase inhibitor cocktail (Roche Diagnostics). Protein concentrations were determined using the Pierce BCA Protein Assay Kit and 13 µg of proteins were run on NuPAGE 4–12% Bis-Tris Gel (Novex by Life Technologies, Carlsbad, CA). The transferred membrane was incubated with the primary antibodies (1:1,000) mouse anti-GFP (Roche Diagnostics) and rabbit anti-α actin (Sigma) at 4 °C overnight. The LI-COR fluorescent secondary antibodies were used (1:10,000) for 1 hour at room temperature. The signal was captured using the Odyssey LI-COR machine (LICOR BIOSCIENCES, Lincoln, NE).

Cell sorting. $Ctns^{-/-}$ fibroblasts were generated from skin biopsies from newborns; 1×10^6 DsRed $Ctns^{-/-}$ fibroblasts were plated for 24 hours before the addition of 6×10^4 CTNSeGFP-fibroblasts in 10 cm culture plates. Cells were cocultured for 14 days. As control, DsRed $Ctns^{-/-}$ fibroblasts were cultured alone. Cells were trypsinized and resuspended in phosphate-buffered saline + 2% fetal bovine serum for sorting. Sorting of the DsRed-expressing cells was performed on a BD FACSAria-I cell sorter (BD Biosciences) prior processing for cystine content.

Statistical analyses. We summarized continuous data as arithmetic means ± SD. Group comparisons of renal function and cystine content parameters were made with parametric analyses of variance, followed by a *t*-test. Associations between transduction efficiency in the blood and transduced cell level in tissues were investigated with linear regressions. All analyses were performed in JMP 8 software (Thomson, Cary, NC). $P < 0.05$ was considered as statistically significant.

ACKNOWLEDGMENTS

We gratefully acknowledge Corinne Antignac (Inserm U983, Paris, France) for providing the *Ctns*$^{-/-}$ mice and Francesco Emma (Bambino Gesù Children's Hospital, Rome, Italy) for the original idea of cross-correction in cystinosis. This work was funded by the Cystinosis Research Foundation and National Institutes of Health RO1-DK090058 and R21-DK090548. No support for this work was derived from any commercial source. The authors declared no conflict of interest.

REFERENCES

1. Krivit, W, Aubourg, P, Shapiro, E and Peters, C (1999). Bone marrow transplantation for globoid cell leukodystrophy, adrenoleukodystrophy, metachromatic leukodystrophy, and Hurler syndrome. *Curr Opin Hematol* **6**: 377–382.
2. Johnston, L (2008). Acute graft-versus-host disease: differing risk with differing graft sources and conditioning intensity. *Best Pract Res Clin Haematol* **21**: 177–192.
3. Pallera, AM and Schwartzberg, LS (2004). Managing the toxicity of hematopoietic stem cell transplant. *J Support Oncol* **2**: 223–37; discussion 237.
4. Cutler, C, Li, S, Ho, VT, Koreth, J, Alyea, E, Soiffer, RJ *et al.* (2007). Extended follow-up of methotrexate-free immunosuppression using sirolimus and tacrolimus in related and unrelated donor peripheral blood stem cell transplantation. *Blood* **109**: 3108–3114.
5. Geyer, MB, Jacobson, JS, Freedman, J, George, D, Moore, V, van de Ven, C *et al.* (2011). A comparison of immune reconstitution and graft-versus-host disease following myeloablative conditioning versus reduced toxicity conditioning and umbilical cord blood transplantation in paediatric recipients. *Br J Haematol* **155**: 218–234.
6. Schleuning, M, Judith, D, Jedlickova, Z, Stübig, T, Heshmat, M, Baurmann, H *et al.* (2009). Calcineurin inhibitor-free GVHD prophylaxis with sirolimus, mycophenolate mofetil and ATG in Allo-SCT for leukemia patients with high relapse risk: an observational cohort study. *Bone Marrow Transplant* **43**: 717–723.
7. Magauran, CE and Salgado, CD (2011). Challenges and advances in infection control of hematopoietic stem cell transplant recipients. *Infect Disord Drug Targets* **11**: 18–26.
8. Wingard, JR, Hsu, J and Hiemenz, JW (2010). Hematopoietic stem cell transplantation: an overview of infection risks and epidemiology. *Infect Dis Clin North Am* **24**: 257–272.
9. Cherqui, S (2012). Cysteamine therapy: a treatment for cystinosis, not a cure. *Kidney Int* **81**: 127–129.
10. Cherqui, S, Kalatzis, V, Trugnan, G and Antignac, C (2001). The targeting of cystinosin to the lysosomal membrane requires a tyrosine-based signal and a novel sorting motif. *J Biol Chem* **276**: 13314–13321.
11. Kalatzis, V, Cherqui, S, Antignac, C and Gasnier, B (2001). Cystinosin, the protein defective in cystinosis, is a H(+)-driven lysosomal cystine transporter. *EMBO J* **20**: 5940–5949.
12. Town, M, Jean, G, Cherqui, S, Attard, M, Forestier, L, Whitmore, SA *et al.* (1998). A novel gene encoding an integral membrane protein is mutated in nephropathic cystinosis. *Nat Genet* **18**: 319–324.
13. Gahl, WA, Thoene, JG and Schneider, JA (2002). Cystinosis. *N Engl J Med* **347**: 111–121.
14. Kleta, R, Bernardini, I, Ueda, M, Varade, WS, Phornphutkul, C, Krasnewich, D *et al.* (2004). Long-term follow-up of well-treated nephropathic cystinosis patients. *J Pediatr* **145**: 555–560.
15. Greco, M, Brugnara, M, Zaffanello, M, Taranta, A, Pastore, A and Emma, F (2010). Long-term outcome of nephropathic cystinosis: a 20-year single-center experience. *Pediatr Nephrol* **25**: 2459–2467.
16. Cherqui, S, Sevin, C, Hamard, G, Kalatzis, V, Sich, M, Pequignot, MO *et al.* (2002). Intralysosomal cystine accumulation in mice lacking cystinosin, the protein defective in cystinosis. *Mol Cell Biol* **22**: 7622–7632.
17. Syres, K, Harrison, F, Tadlock, M, Jester, JV, Simpson, J, Roy, S *et al.* (2009). Successful treatment of the murine model of cystinosis using bone marrow cell transplantation. *Blood* **114**: 2542–2552.
18. Yeagy, BA, Harrison, F, Gubler, MC, Koziol, JA, Salomon, DR and Cherqui, S (2011). Kidney preservation by bone marrow cell transplantation in hereditary nephropathy. *Kidney Int* **79**: 1198–1206.
19. Case, SS, Price, MA, Jordan, CT, Yu, XJ, Wang, L, Bauer, G *et al.* (1999). Stable transduction of quiescent CD34(+)CD38(-) human hematopoietic cells by HIV-1-based lentiviral vectors. *Proc Natl Acad Sci USA* **96**: 2988–2993.
20. Miyoshi, H, Smith, KA, Mosier, DE, Verma, IM and Torbett, BE (1999). Transduction of human CD34+ cells that mediate long-term engraftment of NOD/SCID mice by HIV vectors. *Science* **283**: 682–686.
21. Naldini, L, Blömer, U, Gallay, P, Ory, D, Mulligan, R, Gage, FH *et al.* (1996). *In vivo* gene delivery and stable transduction of nondividing cells by a lentiviral vector. *Science* **272**: 263–267.
22. Verma, IM and Somia, N (1997). Gene therapy – promises, problems and prospects. *Nature* **389**: 239–242.
23. Gonzalez-Murillo, A, Lozano, ML, Montini, E, Bueren, JA and Guenechea, G (2008). Unaltered repopulation properties of mouse hematopoietic stem cells transduced with lentiviral vectors. *Blood* **112**: 3138–3147.
24. Logan, AC, Lutzko, C and Kohn, DB (2002). Advances in lentiviral vector design for gene-modification of hematopoietic stem cells. *Curr Opin Biotechnol* **13**: 429–436.
25. Montini, E, Cesana, D, Schmidt, M, Sanvito, F, Bartholomae, CC, Ranzani, M *et al.* (2009). The genotoxic potential of retroviral vectors is strongly modulated by vector design and integration site selection in a mouse model of HSC gene therapy. *J Clin Invest* **119**: 964–975.
26. Sinn, PL, Sauter, SL and McCray, PB Jr (2005). Gene therapy progress and prospects: development of improved lentiviral and retroviral vectors–design, biosafety, and production. *Gene Ther* **12**: 1089–1098.
27. Biffi, A, De Palma, M, Quattrini, A, Del Carro, U, Amadio, S, Visigalli, I *et al.* (2004). Correction of metachromatic leukodystrophy in the mouse model by transplantation of genetically modified hematopoietic stem cells. *J Clin Invest* **113**: 1118–1129.
28. Kim, EY, Hong, YB, Lai, Z, Cho, YH, Brady, RO and Jung, SC (2005). Long-term expression of the human glucocerebrosidase gene *in vivo* after transplantation

of bone-marrow-derived cells transformed with a lentivirus vector. *J Gene Med* **7**: 878–887.
29. van Til, NP, Stok, M, Aerts Kaya, FS, de Waard, MC, Farahbakhshian, E, Visser, TP *et al.* (2010). Lentiviral gene therapy of murine hematopoietic stem cells ameliorates the Pompe disease phenotype. *Blood* **115**: 5329–5337.
30. Visigalli, I, Delai, S, Politi, LS, Di Domenico, C, Cerri, F, Mrak, E *et al.* (2010). Gene therapy augments the efficacy of hematopoietic cell transplantation and fully corrects mucopolysaccharidosis type I phenotype in the mouse model. *Blood* **116**: 5130–5139.
31. Cartier, N, Hacein-Bey-Abina, S, Bartholomae, CC, Veres, G, Schmidt, M, Kutschera, I *et al.* (2009). Hematopoietic stem cell gene therapy with a lentiviral vector in X-linked adrenoleukodystrophy. *Science* **326**: 818–823.
32. Hacein-Bey-Abina, S, Garrigue, A, Wang, GP, Soulier, J, Lim, A, Morillon, E *et al.* (2008). Insertional oncogenesis in 4 patients after retrovirus-mediated gene therapy of SCID-X1. *J Clin Invest* **118**: 3132–3142.
33. Hippert, C, Dubois, G, Morin, C, Disson, O, Ibanes, S, Jacquet, C *et al.* (2008). Gene transfer may be preventive but not curative for a lysosomal transport disorder. *Mol Ther* **16**: 1372–1381.
34. Bhatia, M, Bonnet, D, Kapp, U, Wang, JC, Murdoch, B and Dick, JE (1997). Quantitative analysis reveals expansion of human hematopoietic repopulating cells after short-term ex vivo culture. *J Exp Med* **186**: 619–624.
35. Dick, JE, Bhatia, M, Gan, O, Kapp, U and Wang, JC (1997). Assay of human stem cells by repopulation of NOD/SCID mice. *Stem Cells* **15** (suppl. 1): 199–203; discussion 204.
36. Di Domenico, C, Villani, GR, Di Napoli, D, Reyero, EG, Lombardo, A, Naldini, L *et al.* (2005). Gene therapy for a mucopolysaccharidosis type I murine model with lentiviral-IDUA vector. *Hum Gene Ther* **16**: 81–90.
37. Kosuga, M, Takahashi, S, Sasaki, K, Li, XK, Fujino, M, Hamada, H *et al.* (2000). Adenovirus-mediated gene therapy for mucopolysaccharidosis VII: involvement of cross-correction in wide-spread distribution of the gene products and long-term effects of CTLA-4Ig coexpression. *Mol Ther* **1**(5 Pt 1): 406–413.
38. Sun, H, Yang, M, Haskins, ME, Patterson, DF and Wolfe, JH (1999). Retrovirus vector-mediated correction and cross-correction of lysosomal alpha-mannosidase deficiency in human and feline fibroblasts. *Hum Gene Ther* **10**: 1311–1319.
39. Tsuji, D, Kuroki, A, Ishibashi, Y, Itakura, T and Itoh, K (2005). Metabolic correction in microglia derived from Sandhoff disease model mice. *J Neurochem* **94**: 1631–1638.
40. Camussi, G, Deregibus, MC, Bruno, S, Cantaluppi, V and Biancone, L (2010). Exosomes/microvesicles as a mechanism of cell-to-cell communication. *Kidney Int* **78**: 838–848.
41. Zomer, A, Vendrig, T, Hopmans, ES, van Eijndhoven, M, Middeldorp, JM and Pegtel, DM (2010). Exosomes: Fit to deliver small RNA. *Commun Integr Biol* **3**: 447–450.
42. Valadi, H, Ekström, K, Bossios, A, Sjöstrand, M, Lee, JJ and Lötvall, JO (2007). Exosome-mediated transfer of mRNAs and microRNAs is a novel mechanism of genetic exchange between cells. *Nat Cell Biol* **9**: 654–659.
43. Belting, M and Wittrup, A (2008). Nanotubes, exosomes, and nucleic acid-binding peptides provide novel mechanisms of intercellular communication in eukaryotic cells: implications in health and disease. *J Cell Biol* **183**: 1187–1191.
44. Aliotta, JM, Sanchez-Guijo, FM, Dooner, GJ, Johnson, KW, Dooner, MS, Greer, KA *et al.* (2007). Alteration of marrow cell gene expression, protein production, and engraftment into lung by lung-derived microvesicles: a novel mechanism for phenotype modulation. *Stem Cells* **25**: 2245–2256.
45. Camussi, G, Deregibus, MC and Tetta, C (2010). Paracrine/endocrine mechanism of stem cells on kidney repair: role of microvesicle-mediated transfer of genetic information. *Curr Opin Nephrol Hypertens* **19**: 7–12.
46. Onfelt, B, Nedvetzki, S, Benninger, RK, Purbhoo, MA, Sowinski, S, Hume, AN *et al.* (2006). Structurally distinct membrane nanotubes between human macrophages support long-distance vesicular traffic or surfing of bacteria. *J Immunol* **177**: 8476–8483.
47. Dull, T, Zufferey, R, Kelly, M, Mandel, RJ, Nguyen, M, Trono, D *et al.* (1998). A third-generation lentivirus vector with a conditional packaging system. *J Virol* **72**: 8463–8471.
48. Zychlinski, D, Schambach, A, Modlich, U, Maetzig, T, Meyer, J, Grassman, E *et al.* (2008). Physiological promoters reduce the genotoxic risk of integrating gene vectors. *Mol Ther* **16**: 718–725.
49. Carbonaro, DA, Jin, X, Petersen, D, Wang, X, Dorey, F, Kil, KS *et al.* (2006). *In vivo* transduction by intravenous injection of a lentiviral vector expressing human ADA into neonatal ADA gene knockout mice: a novel form of enzyme replacement therapy for ADA deficiency. *Mol Ther* **13**: 1110–1120.
50. Kustikova, OS, Modlich, U and Fehse, B (2009). Retroviral insertion site analysis in dominant haematopoietic clones. *Methods Mol Biol* **506**: 373–390.